JCI The Journal of Clinical Investigation

**Amendment history:**
- Corrigendum (December 2010)

# Mammalian target of rapamycin activation underlies HSC defects in autoimmune disease and inflammation in mice

Chong Chen, … , Yang Liu, Pan Zheng

*J Clin Invest.* 2010;120(11):4091-4101. https://doi.org/10.1172/JCI43873.

**Research Article**

The mammalian target of rapamycin (mTOR) is a signaling molecule that senses environmental cues, such as nutrient status and oxygen supply, to regulate cell growth, proliferation, and other functions. Unchecked, sustained mTOR activity results in defects in HSC function. Inflammatory conditions, such as autoimmune disease, are often associated with defective hematopoiesis. Here, we investigated whether hyperactivation of mTOR in HSCs contributes to hematopoietic defects in autoimmunity and inflammation. We found that in mice deficient in *Foxp3* (*scurfy* mice), a model of autoimmunity, the development of autoimmune disease correlated with progressive bone marrow loss and impaired regenerative capacity of HSCs in competitive bone marrow transplantation. Similarly, LPS-mediated inflammation in C57BL/6 mice led to massive bone marrow cell death and impaired HSC function. Importantly, treatment with rapamycin in both models corrected bone marrow hypocellularity and partially restored hematopoietic activity. In cultured mouse bone marrow cells, treatment with either of the inflammatory cytokines IL-6 or TNF-α was sufficient to activate mTOR, while preventing mTOR activation in vivo required simultaneous inhibition of CCL2, IL-6, and TNF-α. These data strongly suggest that mTOR activation in HSCs by inflammatory cytokines underlies defective hematopoiesis in autoimmune disease […]



# Mammalian target of rapamycin activation underlies HSC defects in autoimmune disease and inflammation in mice

Chong Chen,[1] Yu Liu,[1] Yang Liu,[1,2] and Pan Zheng[1,3]

[1]Division of Immunotherapy, Department of Surgery, [2]Department of Internal Medicine, and [3]Department of Pathology, University of Michigan, School of Medicine and Comprehensive Cancer Center, Ann Arbor, Michigan, USA.

**The mammalian target of rapamycin (mTOR) is a signaling molecule that senses environmental cues, such as nutrient status and oxygen supply, to regulate cell growth, proliferation, and other functions. Unchecked, sustained mTOR activity results in defects in HSC function. Inflammatory conditions, such as autoimmune disease, are often associated with defective hematopoiesis. Here, we investigated whether hyperactivation of mTOR in HSCs contributes to hematopoietic defects in autoimmunity and inflammation. We found that in mice deficient in *Foxp3* (*scurfy* mice), a model of autoimmunity, the development of autoimmune disease correlated with progressive bone marrow loss and impaired regenerative capacity of HSCs in competitive bone marrow transplantation. Similarly, LPS-mediated inflammation in C57BL/6 mice led to massive bone marrow cell death and impaired HSC function. Importantly, treatment with rapamycin in both models corrected bone marrow hypocellularity and partially restored hematopoietic activity. In cultured mouse bone marrow cells, treatment with either of the inflammatory cytokines IL-6 or TNF-α was sufficient to activate mTOR, while preventing mTOR activation in vivo required simultaneous inhibition of CCL2, IL-6, and TNF-α. These data strongly suggest that mTOR activation in HSCs by inflammatory cytokines underlies defective hematopoiesis in autoimmune disease and inflammation.**

## Introduction

Mammalian target of rapamycin (mTOR) has emerged as a central regulator for cellular response to environmental cues, such as nutrition, growth factors, and oxygen supplies (1, 2). The potential involvement of mTOR in HSC function was first suggested by the observation that targeted mutation of *Pten*, which is a distant upstream negative regulator of mTOR, resulted in a loss of HSC function (3, 4). mTOR is implicated in *Pten* deficiency–mediated HSC defect, as the defects are reversed by rapamycin (3). Our recent study demonstrated that mTOR hyperactivation abrogates quiescence and function of HSCs by increasing ROS levels (5). More recently, we reported that rapamycin rejuvenates HSCs in and increases lifespan of old mice (6).

Although the consequences of mTOR activation in HSC function are now well established, the pathophysiological conditions that lead to mTOR activation in HSCs remain to be identified. In particular, it is worth considering the possibility that innate or adaptive immune activation may lead to mTOR activation in HSCs. For instance, infectious diseases, such as viral hepatitis, have long been associated with HSC defects (7). In addition, leukocytopenia is an important manifestation of systemic lupus erythematosus (8), although an HSC defect has yet to be established. These data raised an interesting issue as to whether autoimmune diseases and inflammation may cause HSC defects. Moreover, given the impact of mTOR in HSC function, it is intriguing that mTOR activation in HSCs may be responsible for the defective hematopoiesis in both autoimmune diseases and inflammation. Here we use models of autoimmune diseases and endotoxin-induced systemic inflammation to test this hypothesis.

**Conflict of interest:** The authors have declared that no conflict of interest exists.

**Citation for this article:** *J Clin Invest.* 2010;120(11):4091–4101. doi:10.1172/JCI43873.

## Results

*Progressive bone marrow loss and HSC defects in mice with severe autoimmune diseases.* The scurfy mice have severe autoimmune diseases and pancytopenia due to a spontaneous mutation of the forkhead box P3 (*Foxp3*) gene (9, 10). They therefore serve as a valuable model to determine whether and how autoimmune disease causes defective hematopoiesis. We first evaluated their bone marrow cellularity in relation to disease progression. While the 1-week-old scurfy mice that show no sign of autoimmune diseases had normal bone marrow cellularity, a progressive loss of bone marrow cells was observed in the subsequent 3 weeks when autoimmune diseases became severe. The reduction of cellularity was obvious, even after normalization of body weight (Figure 1A). Surprisingly, based on the stringent HSC markers, $Flk2^-lin^-Sca\text{-}1^+c\text{-}kit^+CD150^+CD48^-CD34^-$ (11, 12), we observed a significant increase in the number of the HSCs in the scurfy mice at 3 weeks. This increase was transient, as the number of HSCs was lower in the 4-week-old scurfy mice (Figure 1, B and C). To understand the cellular basis for the increased HSC numbers at 3 weeks, we labeled scurfy mice and their WT littermates with BrdU. At 24 hours after BrdU injection, both scurfy and WT mice had about 60% of bone marrow cells labeled with BrdU. During the same period, about 50% of $Lin^-Sca1^+ckit^+$ (LSK) cells and 40% of HSCs in WT mice were $BrdU^+$. The considerably higher levels of cycling HSCs in young mice, in comparison to what was described in adult mice by others (3) and us (5), are consistent with a previous analysis of HSC cycles (13). In the scurfy mice, about 80% of LSK cells and HSCs were $BrdU^+$ (Figure 1C). Despite an enlargement of the stem cell compartment at 3 weeks, in vitro colony formation unit (CFU) analysis revealed substantial reductions in the progenitor cell activities for all lineages of blood cells (Supplemental Figure 1; supplemental material available online with this article; doi:10.1172/JCI43873DS1).

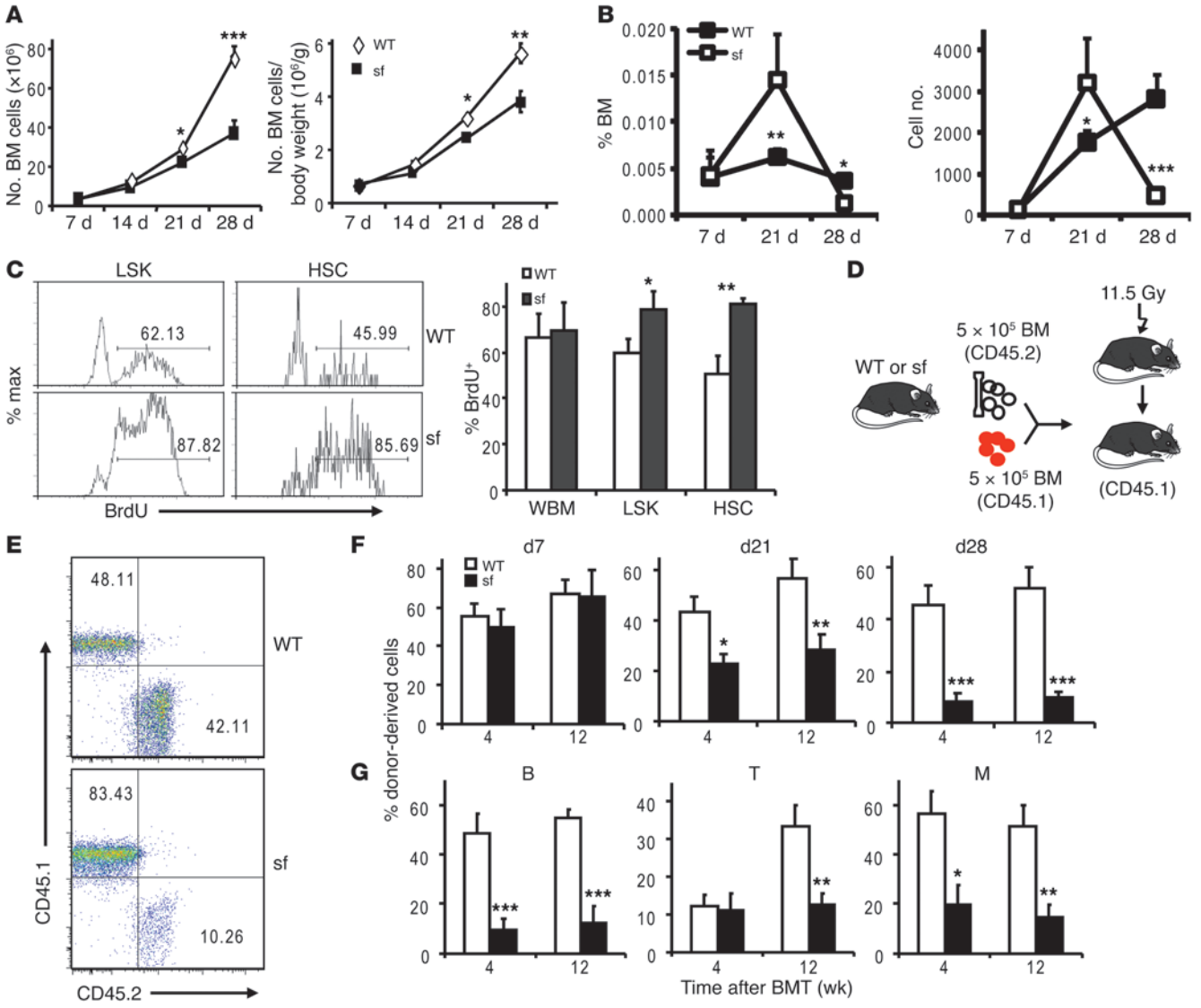


**Figure 1**

Progressive bone marrow hypocellularity and HSC defects in the scurfy mice. (**A**) Bone marrow cellularities of scurfy mice and their littermate controls at days 7, 14, 21, and 28 after birth. Data shown are mean ± SD ($n$ = 4). The absolute number of bone marrow cells in scurfy and WT mice (left) and those after normalization against body weight (right) are shown. (**B**) HSC frequency (left) and numbers (right) in scurfy mice. Data shown are the percentage of Flk2$^-$lin$^-$Sca-1$^+$c-kit$^+$CD34$^-$CD150$^+$CD48$^-$ cells in bone marrow of scurfy mice and their littermate controls at days 7, 21, and 28 (mean ± SD). Each time point involves 3–5 mice per group. (**C**) Hyperproliferation of HSCs in day 21 scurfy (sf) mice. BrdU was labeled in vivo for 24 hours and LSK cells and HSCs were stained with BrdU antibodies. Representative histograms of BrdU staining in gated LSK cell and HSC populations and the percentage of BrdU$^+$ population are shown. Numbers indicate the percentage of BrdU$^+$ cells. WBM, whole bone marrow cells. Data shown are mean ± SD ($n$ = 4). (**D**) Diagram of competitive bone marrow transplantation (BMT). At days 7, 21, and 28, 5 × 10$^5$ bone marrow cells from scurfy mice or those from their littermate controls were mixed with equal number of recipient-type bone marrow cells and transplanted into lethally irradiated CD45.1 C57BL/6 recipients. (**E**) Representative profiles of recipient peripheral blood from 28-day-old donors, evaluated at 12 weeks after reconstitution. Numbers indicate the percentage of donor-derived cells (CD45.2$^+$, right bottom quadrants) or recipient-derived cells (CD45.1$^+$, left top quadrants) in peripheral blood of recipient mice. (**F**) Reconstitution ratios in the recipient peripheral blood by the donor cells were monitored at 4 and 12 weeks after transplant. (**G**) Defective reconstitution in both myeloid (M) (CD11b$^+$) and lymphoid lineages (B220$^+$ for B cells and CD3$^+$ for T cells). The bone marrow used are from 28-day-old mice. Data shown in **F** and **G** are mean ± SD ($n$ = 10) from 2 independent experiments, involving 1 donor and 5 recipients per group. *$P$ < 0.05; **$P$ < 0.01; ***$P$ < 0.001.

To determine the regenerative capacity of HSCs in scurfy mice, we carried out competitive bone marrow transplantation. We transplanted 5 × 10$^5$ bone marrow cells from scurfy or control mice, in conjunction with an equal number of recipient-type bone marrow cells, into lethally irradiated CD45.1 C57BL/6 recipients (Figure 1D). At given time points after transplantation, the percentage of donor-type cells was analyzed using the CD45.2 congenic markers (Figure 1E). As shown in Figure 1F, bone marrow cells from 7-day-old scurfy mice had a comparable reconstitution capacity as those of control mice. However, despite a significant

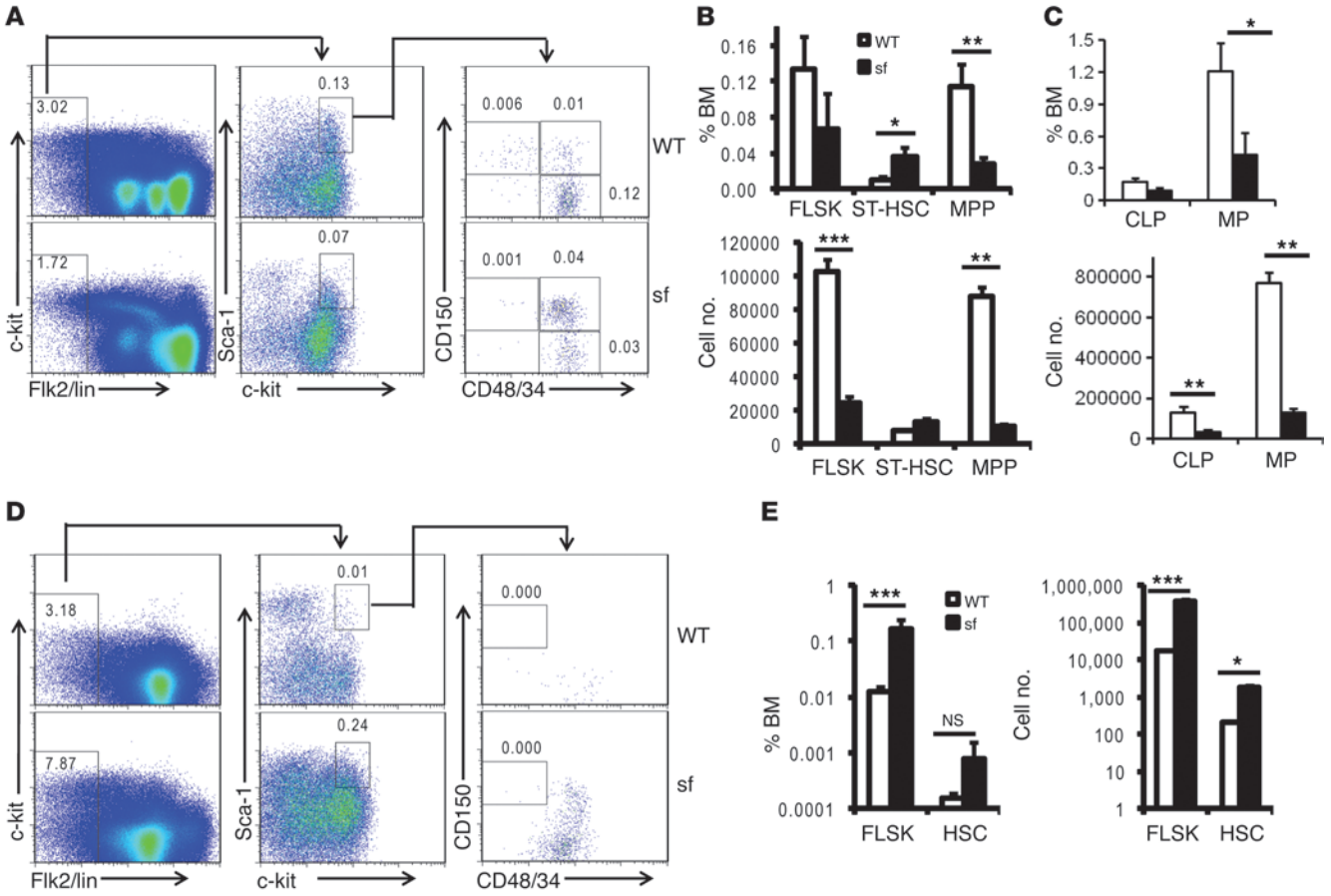


**Figure 2**

HSC and progenitor cell defects in the scurfy mice. Frequencies and numbers of stem and progenitor cells in bone marrow (**A**–**C**) and spleen (**D** and **E**) of the 4-week-old WT mice and scurfy littermates. Representative FACS profiles are presented in **A** and **D**, while summary data are shown in **B**, **C**, and **E**. The percentages of cells are shown in top panels, while the cell numbers are presented in the lower panels. Numbers indicate the percentage of the gated cells in (**A**) total bone marrow or (**D**) spleen. Data shown are mean ± SD ($n = 4$). $^*P < 0.05$; $^{**}P < 0.01$; $^{***}P < 0.001$.

increase of HSC frequency, bone marrow from 3-week-old scurfy mice exhibited significantly reduced HSC activity. The defects were more pronounced in bone marrow from 4-week-old scurfy mice. Defects in production of both B cells and myeloid cells were pronounced at both 4 and 12 weeks after transplantation (Figure 1G). At 12 weeks, it is clear that scurfy bone marrow was substantially defective in T cell reconstitution, although the impact cannot be evaluated at 4 weeks, due to slow T cell reconstitution. Thus, the HSC defects were acquired in the scurfy mice and were progressively associated with the development of autoimmune diseases. Since the defective HSC function was observed in the scurfy mice even when the HSC compartment was enlarged (Figure 1F, middle panel), the defective hematopoiesis was not due to physical elimination of HSCs by the autoreactive T cells or by relocation of HSCs to other compartments. This contention is supported by the fact that, despite the presence of T cells in the bone marrow from the scurfy mice, the cotransplanted recipient-type HSCs were not destroyed (Figure 1, E–G). Since Foxp3 is not expressed in HSCs (Supplemental Figure 2), the HSC defect is unlikely a direct consequence of *Foxp3* mutation. Since the Sca-1 is an activation marker of bone marrow cells (14), we checked whether the increased HSCs in the scurfy mice at 3 weeks merely reflected more activation in the bone marrow cells. As shown in Supplemental Figure 3, the increase in HSC number in the bone marrow was largely unaffected when Sca-1 was dropped as part of the HSC markers.

To characterize the reduction of stem cells and progenitor numbers in 4-week-old scurfy bone marrow, we compared the percentage and number of short-term HSCs (ST-HSCs), $Flk2^-lin^-Sca1^+ckit^+$ (FLSK) cells, multipotent progenitors (MPPs), common lymphoid progenitors (CLPs), and myeloid progenitors (MPs) in the bone marrow and HSCs and MPPs in the spleen. As shown in Figure 2, A–C, and Supplemental Figure 4, a reduction of HSCs was associated with an increase of ST-HSCs. The numbers of FLSK cells, MPPs, CLPs, and MPs were not increased in the bone marrow. Significant increases of FLSK cells and HSCs were observed in the spleen (Figure 2, D and E). Therefore, both increased mobilization and alteration of differentiation of HSCs likely contributed to the reduced HSCs and progenitors in the 4-week-old bone marrow.

*HSCs defects underlie defective hematopoiesis induced by bacterial endotoxin*. We then considered the possibility that the innate immune response may cause HSC defects. To test this hypothesis, we tested whether the broad hematopoietic defects can be induced by LPS, a prototype pathogen-associated molecular pattern (PAMP) that

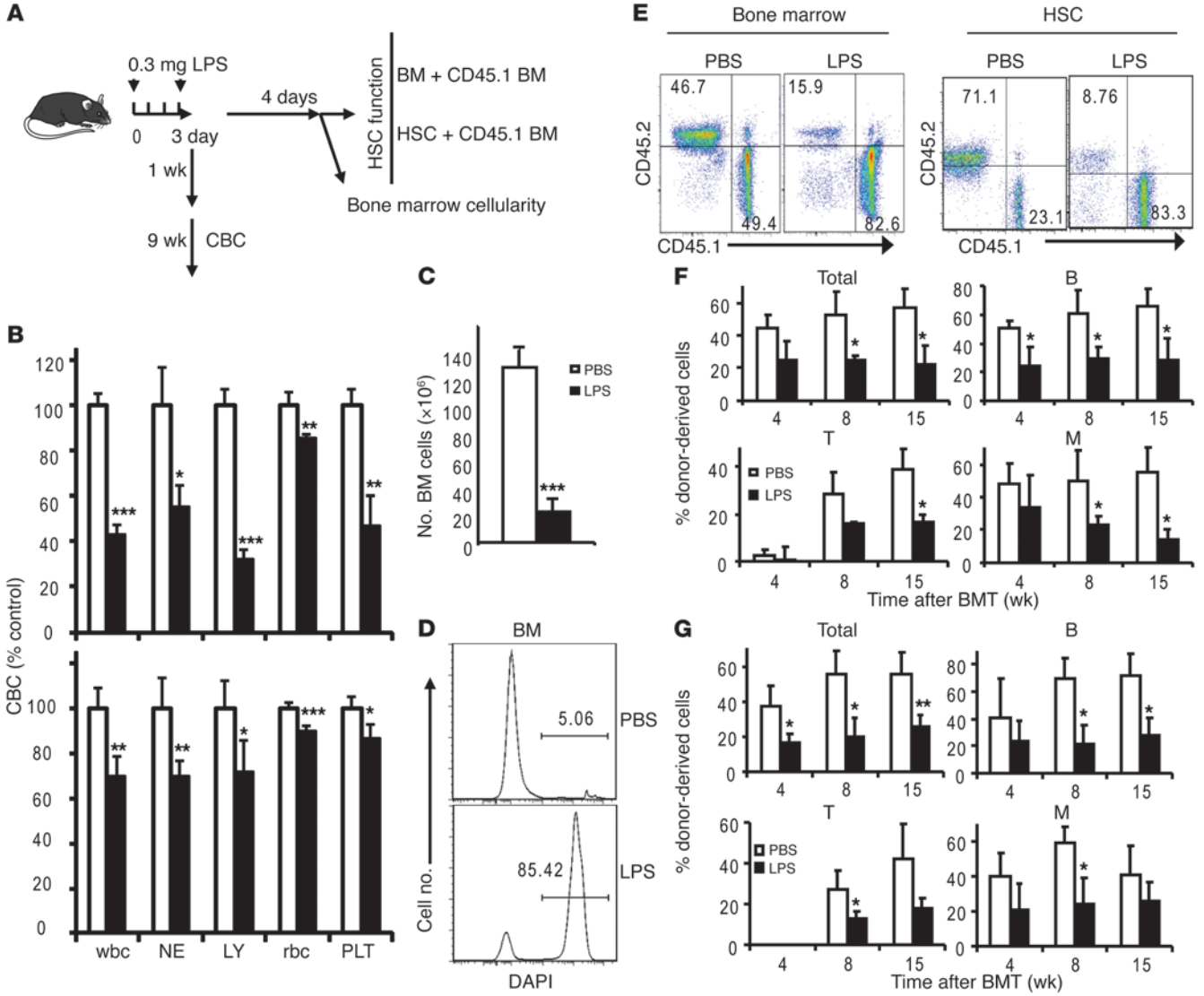


**Figure 3**

LPS causes pancytopenia, bone marrow hypocellularity, and loss of HSC function. (**A**) Diagram of experimental outline. (**B**) Short-term LPS treatment induces pancytopenia. Blood cell counts were measured by CBC test at indicated time points after treatment. Data shown are normalized CBC results of PBS- or LPS-treated mice at 1 week (top) or 10 weeks (bottom) after treatment. NEs, neutrophils; LYs, lymphocytes; PLTs, platelets. Mean ± SD; $n = 10$. (**C**) Bone marrow hypercellularity after LPS treatment. Data shown are (mean ± SD) numbers of bone marrow cells at 1 week after the first LPS treatment ($n = 5$). (**D**) LPS induced massive cell death in bone marrow. Data shown are representative histograms of DAPI staining. Numbers indicate the percentage of DAPI$^+$ cells. (**E**–**G**) LPS treatment impaired the long-term reconstitution capacity of HSCs. (**E**) Representative profiles of donor-type (CD45.2) and recipient-type (CD45.1) blood cells 15 weeks after transplantation. Profiles depicting reconstitution of peripheral blood after transplantation with total bone marrow cells (left) and shows those reconstituted with purified HSCs (right) are shown. Numbers indicate the percentage of donor-derived cells (CD45.2$^+$, left top quadrants) or recipient-derived cells (CD45.1$^+$, right lower quadrants) in peripheral blood of recipient mice. (**F**) $5 \times 10^5$ bone marrow cells from PBS- or LPS-treated mice were mixed with equal numbers of recipient-type bone marrow cells and were transplanted into lethally irradiated CD45.1 C57BL/6 recipients. Summary data at each time point are shown (mean ± SD). (**G**) Fifty FACS-sorted HSCs were mixed with 100,000 recipient-type bone marrow cells. Reconstitution ratios in recipient peripheral blood by the donor cells were monitored at indicated time points after transplant. Total, all leukocytes; B, B220$^+$ B lymphocytes; T, CD3$^+$ T lymphocytes; M, CD11b$^+$ myeloid cells. Data shown are mean ± SD ($n = 10$). *$P < 0.05$; **$P < 0.01$; ***$P < 0.001$.

interacts with TLR4 and triggers inflammatory response (15). As shown in Figure 3A, we injected C57BL/6 mice with lethal doses of LPS and analyzed the complete blood cell count (CBC), bone marrow cellularity, and HSC function. Significant reductions of all lineages of blood cells were observed at 1 or 10 weeks after LPS treatment (Figure 3B). In addition, a massive reduction of bone marrow cellularity was observed after LPS treatment (Figure 3C and Supplemental Figure 5). This reduction was due to the massive cell death of bone marrow cells in the LPS-treated mice (Figure 3D).

We took 2 approaches to determine whether LPS induced HSC defects. First, we mixed bone marrow or HSCs from either vehicle- (PBS-) or LPS-treated mice with recipient-type bone marrow.

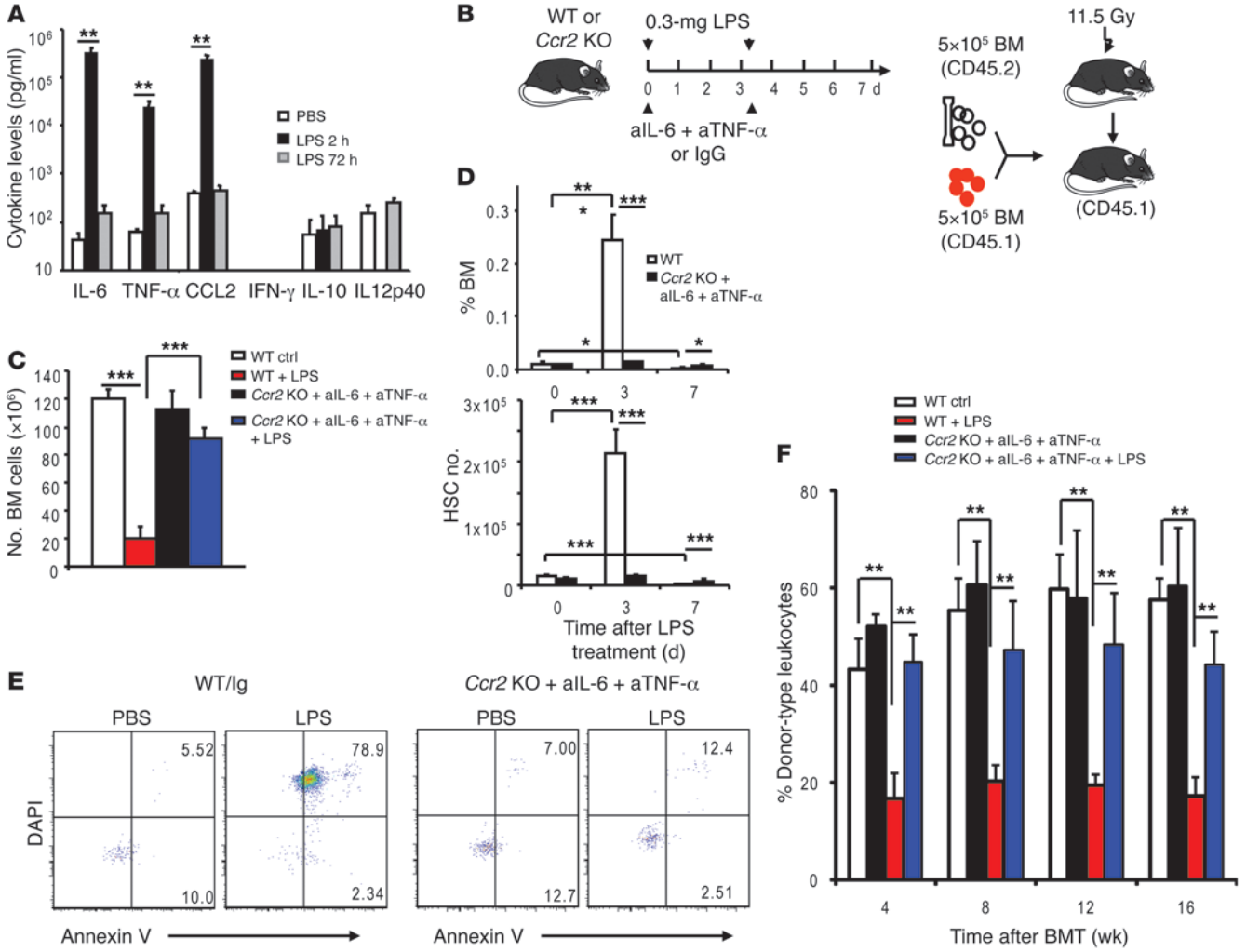


**Figure 4**

IL-6, TNF-α, and CCL2 are responsible for hematopoietic defects in LPS-treated mice. (**A**) The cytokine levels in the plasma of PBS- or LPS-treated mice at 2 or 72 hours after treatment (mean ± SD). (**B**) Diagram of experimental design. Six- to eight-week-old WT or *Ccr2*$^{-/-}$ mice receive LPS on days 0 and 3 (0.3 mg per mice). At both time points, the WT mice also received control mouse IgG, whereas the *Ccr2*$^{-/-}$ mice received equal amounts of mAbs specific for TNF-α and IL-6, respectively. Mice were analyzed on day 0, 3, and 7. aIL-6, anti–IL-6; aTNF-α, anti–TNF-α. (**C**) Involvement of inflammatory cytokines in bone marrow hypocellularity. Data shown are (mean ± SD) bone marrow cell numbers ($n$ = 4). (**D**) The frequency (top) and absolute numbers (bottom) of HSCs in bone marrow after LPS treatment and cytokine blockade. WT mice were treated with control Ig, while *Ccr2*$^{-/-}$ mice received anti–IL-6 and anti-TNF-α mAbs. Mean ± SD. (**E**) Effect of cytokine blockade on apoptosis of HSCs at day 7. Data shown are FACS plots of DAPI and Annexin V staining and represent data from 4 mice per group. Numbers indicate the percentage of apoptotic (Annexin V$^+$ DAPI$^-$) and dead (Annexin V$^+$ DAPI$^+$) cells. (**F**) Role for inflammatory cytokines in LPS-induced HSC defects. WT or anti–IL-6 and anti–TNF-α–treated *Ccr2*$^{-/-}$ mice were treated with PBS or LPS twice. Four days after the second treatment, 5 × 10$^5$ bone marrow cells were mixed with equal numbers of recipient-type (CD45.1) bone marrow cells and were transplanted into lethally irradiated CD45.1 C57BL/6 recipients. Reconstitution ratios in the recipient peripheral blood by the donor cells were monitored at 4, 8, and 12 weeks after transplantation. Data shown are mean ± SD ($n$ = 10). *$P$ < 0.05; **$P$ < 0.01; ***$P$ < 0.001.

Although the HSCs in the PBS group were as efficient as the recipient-type bone marrow in hematopoiesis, those from the LPS group were much less functional (Figure 3E). The defects were observed in multiple lineages and persisted over the 15 weeks studied (Figure 3F). Since the defects were long lasting and occurred in T, B, and myeloid cells, they likely reflect a defective HSC function. Second, to directly demonstrate the HSC defects, we used 50 FACS-sorted HSCs from the 2 groups to compete with 10$^5$ recipient-type bone marrow cells. As shown in Figure 3G, the purified HSCs from the LPS-treated mice were significantly less potent in hematopoiesis. Again, the defects were manifested in the numbers of total leukocytes as well as T, B, and myeloid cells.

*Multiple inflammatory cytokines are responsible for LPS-induced HSC defects.* LPS may either directly inactivate HSCs or do so by inducing inflammatory cytokines. As shown in Figure 4A, high levels of IL-6, TNF-α, or CCL2 were found 2 hours after LPS treatment. In contrast, no induction of IFN-γ, IL-10, and IL12p40 was observed. The elevation was not long lasting, as the cytokine levels at 72 hours after LPS treatment largely returned to baseline. To address the potential role for the inflammatory cytokines, we used antibodies

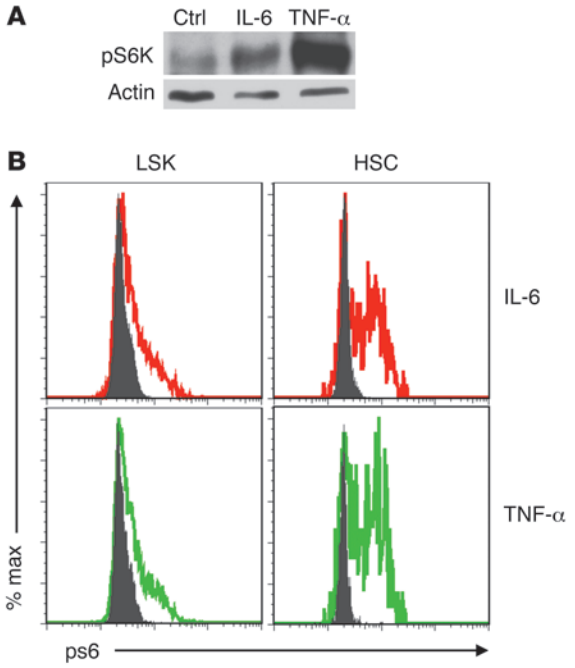


**Figure 5**

IL-6 and TNF-α activate the mTOR pathway in HSCs. c-kit+ bone marrow cells were isolated from 2- to 3-month-old WT C57BL/6 mice and cultured with or without IL-6 or TNF-α for 30 minutes. mTOR activity was measured in the total c-kit+ bone marrow cells by the level of pS6K using Western blot (**A**) and in the LSK cells and HSC populations using flow cytometry (**B**). The data have been repeated in 3 independent experiments.

to block the effect of IL-6 and TNF-α. In addition, we used mice with a targeted mutation of the *Ccr2* gene that encodes the dominant CCL2 receptor to test the impact of CCL2 (16). Because blocking individual cytokines had no appreciable effect in preventing bone marrow hypocellularity (Supplemental Figure 5), we treated *Ccr2*-deficient mice with a combination of anti–IL-6 and anti–TNF-α mAbs in order to block all 3 cytokines simultaneously (Figure 4B). This combination largely reversed the massive loss of bone marrow cellularity (Figure 4C). Furthermore, LPS treatment caused a large increase in the number of cells with HSC phenotypes on day 3 (Figure 4D). This increase was not due to increased bone marrow activation marker Sca-1 (Supplemental Figure 6). However, most of the HSCs had undergone apoptosis, as revealed by their staining to Annexin V and permeability to the nuclear dye DAPI (Figure 4E). By day 7, the number of HSCs in the LPS-treated mice was lower than that in the PBS-treated mice (Figure 4D). The rise and fall of HSC numbers was largely eliminated in the anti–TNF-α/IL-6–treated *Ccr2*-deficient mice (Figure 4D). Likewise, apoptosis of HSCs was abrogated by blocking the 3 cytokines (Figure 4E).

To test the function of HSCs, we carried out competitive bone marrow transplantation (Figure 4B). As shown in Figure 4F, blocking the 3 cytokines reversed the defects in bone marrow cells from the LPS-treated mice. The impact was observed at all time points tested (Figure 4F) and found in T and B cell lineages (Supplemental Figure 7).

*Inflammatory cytokines inactivate HSCs by mTOR-dependent mechanisms*. Given our previous studies on the impact of mTOR activation on HSC function (5, 6), we wondered whether the inflammatory cytokines may inactivate HSCs by stimulating mTOR. To test this possibility, we treated cKit+ bone marrow cells from WT mice with either IL-6 or TNF-α. The dose used (5 ng/ml) was no higher than what was observed in the LPS-treated mice (Figure 3A). As shown in Figure 5A, treatment for 30 minutes with either cytokine substantially induced phosphorylation of S6 kinase (S6K), a downstream target of mTOR. To confirm that mTOR activation occurred in HSCs, we analyzed the pS6 levels in the LSK cells and HSCs using flow cytometry. As shown in Figure 5B, both cytokines induced mTOR activation in both LSK cells and HSCs. However, the percentage of pS6+ cells was higher in HSCs than that in LSK cells. These data demonstrated that either IL-6 or TNF-α was sufficient to activate mTOR in HSCs.

To determine potential contribution of mTOR activation to HSC defects in LPS-treated mice, we tested whether mTOR activation in HSCs was induced by LPS in vivo. At 2 hours after LPS treatment, a substantial increase of pmTOR (Figure 6, A and B) and pS6 (Figure 6, C and D) was observed in total bone marrow cells, including LSK cells and HSCs. Based on mean fluorescence intensity, the increase in total bone marrow cells (<1-fold increase) was substantially less than that in either LSK cells or HSCs (2- to 3-fold increase in pmTOR and 7- to 8-fold increase in pS6). Importantly, the inflammatory cytokines IL-6, TNF-α, and CCL2 played a critical role in mTOR activation, as the induction of pS6 was abrogated when the 3 cytokines were simultaneously blocked (Figure 6, E and F).

To determine the role for mTOR activation in LPS-induced hematopoietic defects, we injected rapamycin in conjunction with LPS, starting 1 day prior to LPS treatment (Figure 7A). Although this treatment did not reduce the production of IL-6, TNF-α, and CCL2 (Figure 7B), rapamycin essentially abrogated the LPS-induced bone marrow hypocellularity (Figure 7C). Corresponding to restoration of cellularity, rapamycin also prevented the massive apoptosis in bone marrow cells (Figure 6D). We then used competitive bone marrow transplantation to determine whether rapamycin restored the hematopoietic activity of bone marrow from LPS-treated mice (Figure 7A). As shown in Figure 7E, rapamycin partially abrogated the inhibition of hematopoietic activity by LPS, as measured by either total leukocytes or B cells at either 4 or 10 weeks after transplantation. Since T cell development is usually slower, the effect of rapamycin was observed at 10 weeks only. Although a significant effect was observed for myeloid lineage at 4 weeks, the trend observed at 10 weeks is not statistically significant.

*Hyperactive mTOR underlies HSC defects in scurfy mice*. Since the levels of inflammatory cytokines were also very high in the scurfy mice (Supplemental Figure 8), we tested whether the HSC defects in the mice described in Figure 1 were also due to the hyperactive mTOR pathway. Again, we determined the mTOR status in the HSCs using flow cytometric analysis of phosphorylation of mTOR and S6. As shown in Figure 8A and Supplemental Figure 9, the mean fluorescence intensities of both pmTOR and pS6 were significantly increased in the scurfy HSCs in comparison with those of the WT HSCs. Consistent with our previous observation, mTOR activation was associated with increased expression of senescence marker gene cyclin-dependent kinase inhibitor 2A (*p16$^{ink4a}$*) (Supplemental Figure 10).

In order to determine whether mTOR activation is the underlying cause of the HSC defects in the scurfy mice, we treated 2-week-old scurfy mice with rapamycin at a daily dose of 4 mg/kg for 7 days and tested the effect of rapamycin on lifespan and hematopoiesis of the scurfy mice as well as the function of

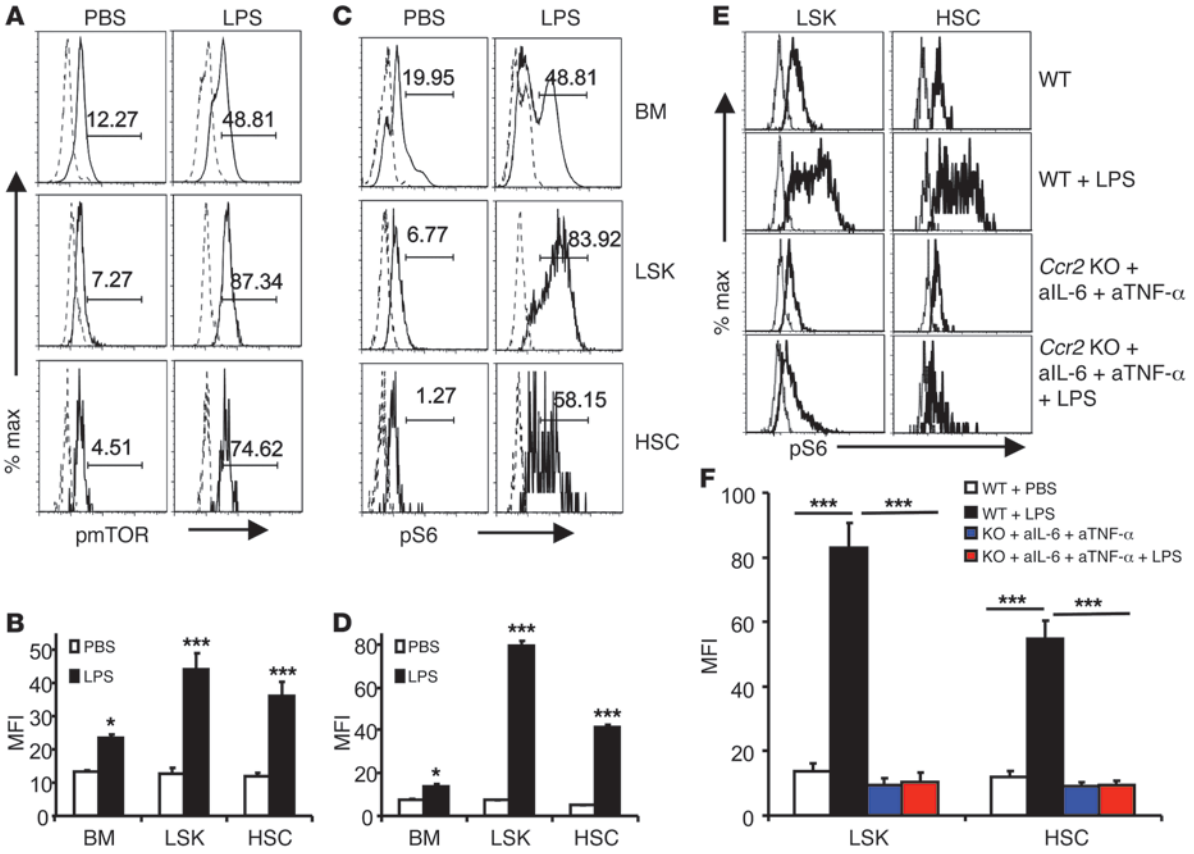


**Figure 6**

An essential role for inflammatory cytokines in mTOR activation in HSCs. (**A**–**D**) LPS induces phosphorylation of mTOR and S6 proteins. C57BL/6 mice were treated with PBS (control) or 0.3 mg LPS. Two hours after treatment, bone marrow cells were harvested and the levels of phosphorylated mTOR (**A** and **B**) and phosphorylated S6 (**C** and **D**) in whole bone marrow cells, LSK cells, and HSCs were measured by flow cytometry. (**A** and **C**) Representative FACS profiles. Solid lines depict fluorescence of samples stained with either anti-pmTOR (**A**) or pS6 (**C**), while the dotted lines depict those of isotype control-stained samples. Number indicate (**A**) the percentage of pmTOR$^+$ cells and (**C**) the percentage of pS6$^+$ cells. (**B** and **D**) Summary data of levels of pmTOR (**B**) and pS6 (**D**). (**E** and **F**) Inflammatory cytokines are essential for mTOR activation in LSK cells and HSCs. (**E**) Representative histograms. (**F**) Summary data involving 5 mice per group. Data shown in **B**, **D**, and **F** are mean ± SD of the mean fluorescence intensity. $n = 5$. $^*P < 0.05$; $^{***}P < 0.001$.

HSCs in competitive bone marrow transplantation (Figure 8B). As shown in Figure 8C, 1 week of rapamycin treatment significantly extended the lifespan of scurfy mice, which is consistent with a report involving 2 immunodeficiency polyendocrinopathy, enteropathy, X-linked syndrome (IPEX) patients (17). However, this treatment inhibited neither the production of inflammatory cytokines (Supplemental Figure 8A) nor lymphoproliferation as manifested by splenomegaly (Supplemental Figure 8B) and the adenopathy (our unpublished observations). Therefore, a therapeutic benefit can be achieved without overt inhibition of inflammation and lymphoproliferation.

At 2 weeks after the treatments, the bone marrow cells were isolated and tested for HSC function. As shown in Figure 8D, rapamycin treatment significantly increased the bone marrow cellularity. In addition to the total numbers of leukocytes, a remarkable reduction of B cells was observed in the scurfy bone marrow. This is also substantially rescued by rapamycin treatment (Figure 8, E and F). Further, the production of immature (Ter119$^+$CD71$^+$) and mature (Ter119$^+$CD71$^-$) erythroblasts was also restored by rapamycin treatment. To determine whether rapamycin restored the HSC function in the scurfy mice, the bone marrow of vehicle- or rapamycin-treated mice was mixed with an equal number of recipient-type bone marrow cells and transplanted into lethally irradiated CD45.1 recipients. The PBLs were analyzed at 3 months after bone marrow transplantation. As shown in Figure 8G, the frequency of donor-type nucleated blood cells increased by about 6 fold in the rapamycin group. Substantial increases were found in all cell lineages tested, including T, B lymphocytes, and myeloid cells (Supplemental Figure 11). Therefore, a short-term rapamycin treatment restored the long-term HSC function of the scurfy mice in the new hosts.

## Discussion

It is well established that hematological abnormalities are associated with infections (18), inflammation (19), and autoimmune diseases (20). However, whether and how these pathophysiological conditions affect HSC function remain unresolved. Here, we used models for both autoimmune diseases and inflammation to demonstrate 3 intrinsic links among HSC defects and these conditions.

First, our data demonstrate that autoimmune diseases cause HSC defects. Traditionally, immunologists have focused on

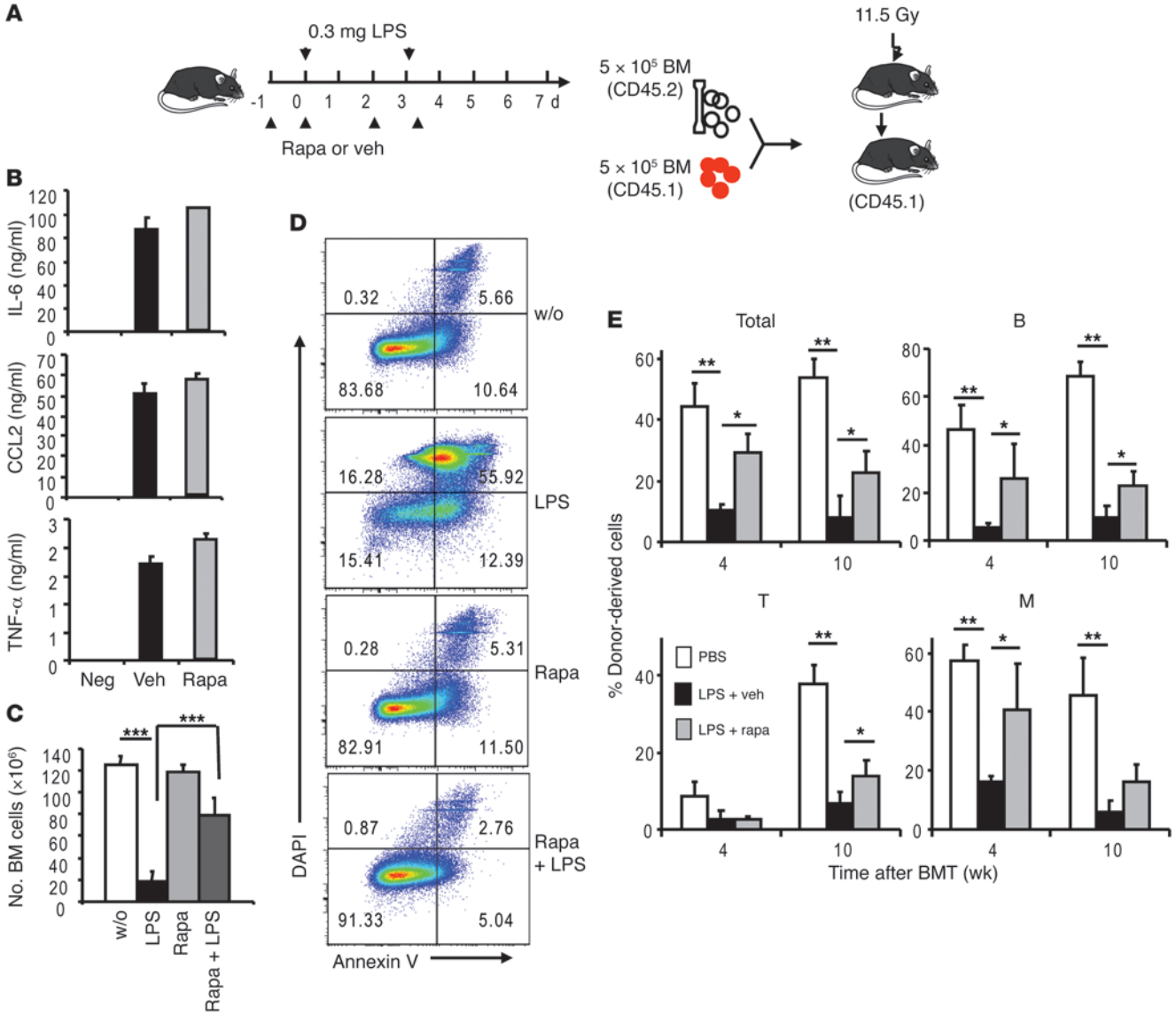


**Figure 7**

Rapamycin rescues LPS-induced defects in bone marrow. (**A**) Diagram of experimental design. Mice that received LPS on days 0 and 3 were treated with either vehicle (veh) or rapamycin (rapa) on days –1, 0, 2, and 3. Bone marrow cells were analyzed on day 7. (**B**) Rapamycin did not reduce levels of inflammatory cytokines in the plasma. Data shown are mean ± SD of plasma levels of IL-6, TNF-α, and CCL2 at 2 hours after LPS treatment ($n = 5$). Mice in the "Neg" group received PBS. Mice in the vehicle or rapamycin groups received LPS with either vehicle or rapamycin treatment. (**C**) Rapamycin prevented LPS-induced bone marrow hypocellularity. Data shown are mean ± SD of the number of bone marrow cells ($n = 5$). Mice in the "w/o" or LPS groups received PBS or LPS and were treated with vehicle. Mice in the rapamycin and rapamycin plus LPS groups received PBS or LPS and were treated with rapamycin. (**D**) Rapamycin prevented apoptosis of bone marrow cells induced by LPS. Data shown are representative FACS profiles of an experiment involving 5 mice per group. Numbers indicate the percentage of gated cells in bone marrow. (**E**) Inhibition of mTOR by rapamycin prevented LPS-induced loss of HSC function. 5 × $10^5$ bone marrow cells, mixed with equal number of recipient-type bone marrow cells, were transplanted into lethally irradiated CD45.1 C57BL/6 recipients. Reconstitution ratios in the recipient peripheral blood by the donor cells were monitored at indicated time points after transplant. M, Mac-1$^+$ myeloid cells. Data shown are mean ± SD ($n = 10$). *$P < 0.05$; **$P < 0.01$; ***$P < 0.001$.

both innate and adaptive responses of mature leukocytes in autoimmune diseases. How the stem cells may respond in this setting has not been systematically studied. Here, we demonstrated that scurfy mice, which have spontaneous inactivation of Foxp3$^+$ Tregs and fatal autoimmune diseases, exhibit significant HSC defects when tested in competitive bone marrow transplantation. Since Foxp3 is not expressed in HSCs (Supplemental Figure 2), it is likely that the HSC defects are secondary to autoimmune diseases.

Because of the increased burden of autoreactive T cells or autoantibodies in the scurfy mice (10, 21, 22), it may be tempting to suggest that HSCs were destroyed by self-reactive T cells or autoantibodies. However, since recipient-type bone marrow cells functioned normally when cotransplanted into irradiated

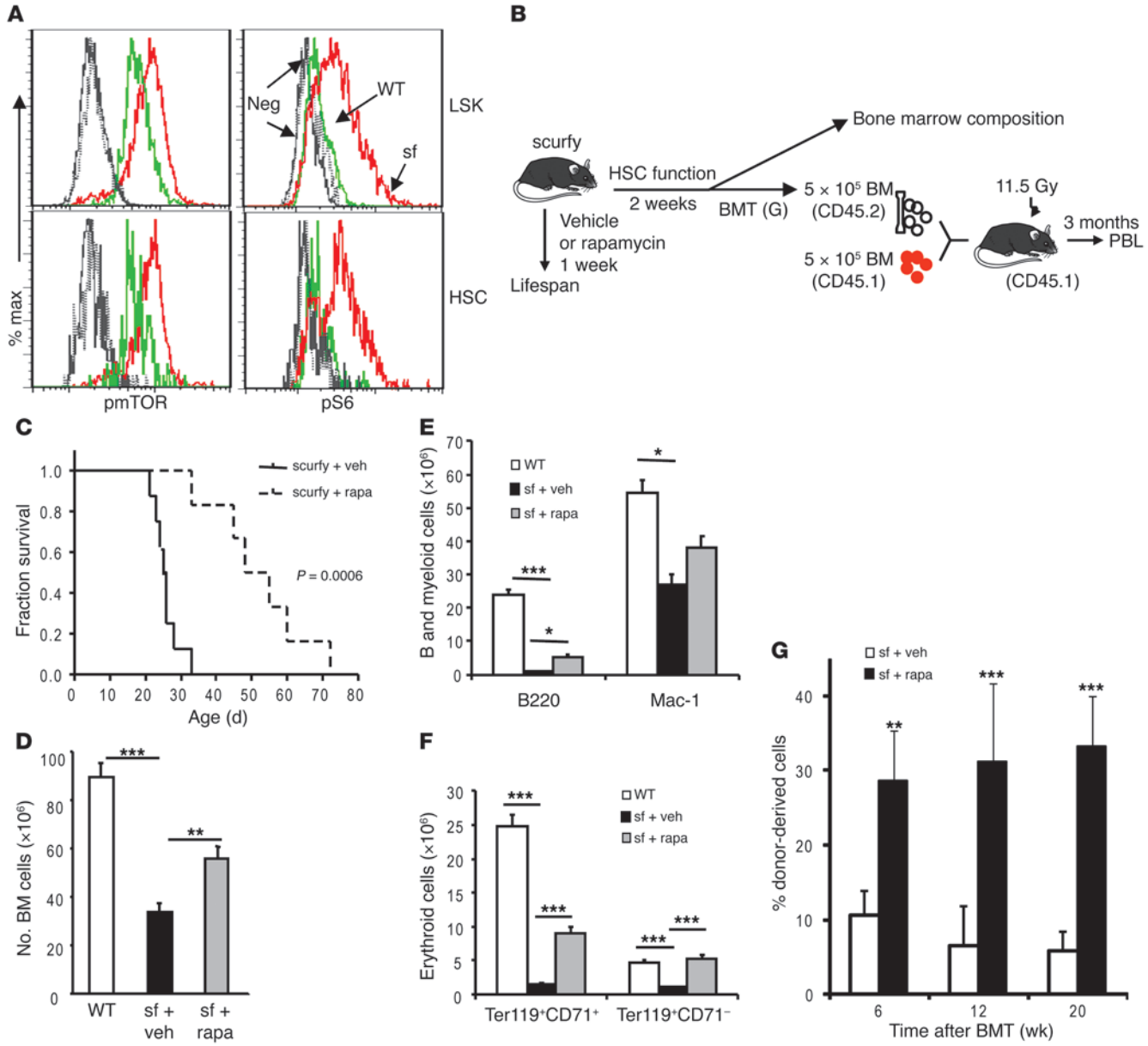


**Figure 8**

Hyperactivity of mTOR in HSCs causes defective hematopoiesis in the scurfy mice. (**A**) Hyperactivation of the mTOR pathway in HSCs. Bone marrow cells from 3-week-old scurfy mice and their littermate controls were stained with antibodies specific for phosphorylated mTOR and phosphorylated S6. Data shown are representative histograms from 2 independent experiments, each involving 2 mice per group. (**B**–**G**) Rapamycin treatment increased lifespan, reduced abnormalities in hematopoiesis, and restored HSC function in the scurfy mice. (**B**) Diagram of experiments. The 2-week-old scurfy mice were treated for either 1 (survival analysis) or 2 weeks (bone marrow composition and transplantation) with rapamycin (4 mg/kg/injection, every other day). (**C**) Short-term rapamycin treatment substantially increased lifespan of the scurfy mice. After 1 week of treatment, the mice were left untreated for observation until they were moribund. The vehicle- and rapamycin-treated groups were compared by Kaplan-Meier survival analysis, and the statistical significance was determined by log-rank test (mean ± SD; $n = 8$ for the vehicle group and $n = 6$ for the rapamycin group). (**D**–**G**) Rapamycin treatment partially restored bone marrow cellularity (**D**), B and myeloid cells (**E**), and erythroid lineage (**F**) development in bone marrow. Data in **D**–**G** are mean ± SD ($n = 3$). (**G**) Short-term rapamycin treatment in the scurfy mice increased their HSC function. Data shown are the percentage of CD45.2$^+$ donor (scurfy) bone marrow–derived cells in the peripheral blood at various time points after bone marrow transplantation. Data shown are mean ± SD ($n = 15$) from 3 independent donors per group. $^*P < 0.05$; $^{**}P < 0.01$; $^{***}P < 0.001$.

host with scurfy bone marrow cells, it is unlikely either antibody-producing cells or autoreactive T cells in the scurfy bone marrow can prevent the function of normal HSCs. Furthermore, at 3 weeks, when the number of HSCs in the bone marrow was at least 10-fold higher in the scurfy mice than in WT mice, the scurfy bone marrow cells showed significant defects in hematopoiesis in transplantation assay. Therefore, hematopoietic defects are not due to physical elimination of HSCs. It is

more plausible that the environment in the autoimmune mice causes functional inactivation of HSCs.

The causative relationship between autoimmune diseases and HSC defects demonstrated herein may explain frequent leucopenia in systemic lupus erythematosus (8). Moreover, AA, which is a well-established HSC disease, is believed to be due to autoimmune diseases, because the majority of the patients respond to immune suppression (23–25). It is of note that given the potential contribution of homeostatic proliferation to autoimmune diseases (26, 27), defective hematopoiesis and autoimmune diseases may form a vicious cycle to the detriment of the host. As such, breaking this cycle may have significant therapeutic implications for both autoimmune diseases and hematological defects.

Second, we demonstrated a direct link between inflammatory cytokines and HSC defects. A potential link between inflammation and HSC function has not been established. A recent study showed that LPS from *Pseudomonas aeruginosa* caused a block in generation of common progenitors for myeloid cells. Moreover, a germline mutation of TLR4 prevented common MP defects in LPS-treated mice (28). A different regiment of LPS treatment has lead to defects in CLPs (29). Here, we have shown that LPS caused long-lasting HSC defects by inducing IL-6, TNF-α, and Ccl2. As a consequence, reconstitutions of both the lymphoid and myeloid compartments are adversely affected.

Both infection and tissue injuries trigger production of inflammatory cytokines through recognition of either PAMPs or danger-associated molecular patterns (DAMPs) (30, 31). Host responses to DAMPs are selectively regulated by CD24-Siglec G/10 interaction (32, 33). The abnormal production of PAMPs or DAMPs or interruption of CD24-Siglec G/10 interaction may all create a proinflammatory environment. Therefore, the link between inflammatory cytokines and HSC defects, as uncovered here, may have broad significance on a variety of pathophysiological conditions. Since mTOR activation can be induced by a multitude of inflammatory cytokines, and since the increase of inflammatory cytokines is found in both experimental models, it is possible that these pathological conditions involve similar mechanisms. However, due to higher levels and the more transient nature of inflammatory cytokines, the effect of LPS is more acute.

Last, but not the least, our data demonstrated that both inflammation and autoimmune diseases induce HSC defects through mTOR activation. In both models, we observed a transient expansion and decline in HSC number, which is reminiscent of the observations made in HSCs with mutations of *Pten* and *Tsc1*, 2 upstream negative regulators of mTOR (3–5). The functional defects in HSCs are also reminiscent of the *Tsc*- and *Pten*-deficient HSCs, although the phenotype in the *Pten*-deficient HSCs is complicated by development of malignancy and genetic instability (3–5). The critical role of mTOR activation in HSC defects is confirmed by the effect of rapamycin. However, since all experimental conditions activate or inactivate mTOR in other cell types, one may envisage that rapamycin inhibits production of inflammatory cytokines by other cells, which in turn inactivates HSCs by mTOR-independent mechanisms. Therefore, it is formally possible that the HSC defects are due to HSC-extrinsic activation of mTOR. We consider this very unlikely, as our data indicated that rapamycin has no effect on the production of inflammatory cytokines in these settings.

We have recently reported that mTOR activation is the underlying cause of HSC senescence in the old mice (6). The stimuli that cause mTOR activation in the old mice have not been identified. Given the increased levels of inflammatory cytokines in the elderly, it is of interest to consider inflammation as a cause of HSC aging. In this regard, it is of interest that HSCs from autoimmune mice also exhibit higher levels of senescence marker $p16^{INK4a}$. Taken together, our data suggest that mTOR activation underlies HSC defects associated with infection, inflammation, autoimmune diseases, and aging. This conclusion may have interesting implications for the treatment of hematological abnormalities.

## Methods

*Mice*. C57BL/6 Ly5.1 (CD45.2) C57BL/6 Ly5.2 (CD45.1) mice were purchased from the National Cancer Institute. The scurfy mice were obtained from The Jackson Laboratory. The *Ccr2*$^{-/-}$ mice (16) were obtained from the University of Michigan Animal Core. *FoxP3*$^{EGFP}$ mice that express both FoxP3 and EGFP under the endogenous regulatory sequence of the FoxP3 locus have been described previously (34) and have been provided by T.A. Chatila (Department of Pediatrics, UCLA, Los Angeles, California, USA). All the mice were kept in the Unit of Laboratory Animal Facility at University of Michigan. All procedures involving experimental animals were approved by the University Committee on the Use and Care of Animals at the University of Michigan.

*LPS, antibodies, and rapamycin treatment*. LPS from *Escherichia coli* 055:B5 (Sigma-Aldrich) was resuspended in 1x PBS at 2 mg/ml. Mice were treated with 0.3 mg once or twice, as indicated, by intraperitoneal injection. Rapamycin (Sigma-Aldrich) was reconstituted in absolute ethanol at 10 mg/ml and diluted in 5% Tween-80 (Sigma-Aldrich) and 5% PEG-400 (Hampton Research). Mice received 4 mg/kg rapamycin by intraperitoneal injection every other day (5). Control IgG or anti–TNF-α (35) and anti–IL-6 mAb (LS-C7955, LifeSpan Bio.) were injected intraperitoneally (100 μg/mouse) on days 0 and 3 of LPS injection.

*BrdU incorporation*. BrdU (Sigma-Aldrich) was injected intraperitoneally into adult mice at 100 mg/kg body weight. Mice were then given 1 mg/ml BrdU in the drinking water for 24 hours before sacrifice for analysis. The BrdU staining kit (BD Biosciences) was used according to the manufacturer's instructions.

*Transplantation assays*. Eight-week-old congenic recipient mice were lethally irradiated with a Cs-137 x-ray source, delivering 0.97 Gy per minute, for a combined 11.5 Gy, that were delivered 4 hours apart. Bone marrow cells of the donor type were mixed with competitive recipient-type bone marrow cells and were then transplanted into recipients by injection through the retro-orbital venous sinus. Reconstitutions were measured using flow cytometry of blood from the tail vein at the time points indicated. The red blood cells were lysed using ammonium chloride/potassium bicarbonate buffer before staining.

*Flow cytometry*. Bone marrow cells were flushed out from the long bones (tibias and femurs) by using a 25-gauge needle with 1x HBSS, without calcium or magnesium (Invitrogen), supplemented with 2% heat-inactivated fetal bovine serum. For flow cytometry and purification of HSCs, the immunophenotype $Flk2^{-}lin^{-}Sca\text{-}1^{+}c\text{-}kit^{+}CD34^{-}CD150^{+}CD48^{-}$ was used, and the LSK cell population was marked as $lin^{-}Sca\text{-}1^{+}c\text{-}kit^{+}$. Lineage markers included B220, CD3, Gr-1, Mac-1, and Ter119. The anti-CD150 antibody was purchased from BioLegend, and all other antibodies were obtained from BD Biosciences. For intracellular staining, cells were first stained with indicated surface markers, then fixed with Fix buffer (BD Biosciences) for 2 hours at 4°C, followed by permeate buffer for 10 minutes at room temperature, and then refixed for 10 minutes. pmTOR antibodies (Cell Signaling Technology) were diluted at 1:100 and Alexa Fluor 488–conjugated pS6 antibodies (Cell Signaling Technology) and FITC-conjugated p16Ink4a

antibodies (Santa Cruz Biotechnology Inc.) were diluted at 1:10 and incubated overnight at 4°C. FITC-conjugated secondary antibodies (Jackson ImmunoResearch Laboratories Inc.) for pmTOR staining were diluted at 1:100 and incubated for 2 hours at 4°C. The Foxp3 Staining Kit (eBioscience) was used for Foxp3 staining. Flow cytometry analysis was performed on BD LSR II (BD Biosciences). FACS sorting was performed on BD FACSDiva (BD Biosciences).

*Real-time PCR*. LSK cells and HSCs were purified by FACS sorting, and RNA was isolated with TRIzol (Invitrogen) and further purified using the RNeasy Kit (Invitrogen). cDNA was made from purified RNA with SuperScript III (Invitrogen). Real-time PCR was performed on the 7500 Real-Time PCR System (Applied Biosystems). The sequences of RT-PCR primers for p16Ink4a were as follows: forward, 5′-TTCTTGGTGAAGTTCGTGCGATCC-3′, and reverse, 5′-TTGAGCAGAAGAGCTGCTACGTGA-3′.

*CFU assay*. Total bone marrow cells isolated from 21-day-old WT or scurfy mice were plated into MethoCult GFM3434 (StemCell Technologies Inc.) and cultured for 12 days before being counted under a microscope (CKX31; Olympus).

*Western blot*. c-Kit–positive cells were isolated from C57BL/6 mice bone marrows with biotin-conjugated anti–c-Kit antibody (BD Biosciences) and MACS separation column. The c-Kit–positive cells were lysed with lysis buffer (Cell Signaling) and analyzed using SDS-PAGE and Western blot with anti–phospho-S6K (Cell Signalling) and anti-actin (Abcam) antibodies.

*Statistics*. A paired 2-tailed Student's *t* test was used to compare the sorted bone marrow cells from WT or scurfy mice and to compare the peripheral blood cells or bone marrow cells from mice treated with LPS or PBS. *P* values of less than 0.05 were considered significant.

## Acknowledgments

We thank Shenghui He and Linhua Vatan for technical help and Darla Kroft for critical reading of the manuscript. This study was supported by grants from National Institute of Health and US Department of Defense.

Received for publication May 28, 2010, and accepted in revised form August 25, 2010.

Address correspondence to: Pan Zheng or Yang Liu, BSRB 2059, 109 Zina Pitcher Place, Ann Arbor, Michigan 48109, USA. Phone: 734.615.3158; Fax: 734.763.2162; E-mail: panz@umich.edu (P. Zheng) or yangl@umich.edu (Y. Liu).

1. Inoki K, Corradetti MN, Guan KL. Dysregulation of the TSC-mTOR pathway in human disease. *Nat Genet*. 2005;37(1):19–24.
2. Inoki K, Guan KL. Complexity of the TOR signaling network. *Trends Cell Biol*. 2006;16(4):206–212.
3. Yilmaz OH, et al. Pten dependence distinguishes haematopoietic stem cells from leukaemia-initiating cells. *Nature*. 2006;441(7092):475–482.
4. Zhang J, et al. PTEN maintains haematopoietic stem cells and acts in lineage choice and leukaemia prevention. *Nature*. 2006;441(7092):518–522.
5. Chen C, Liu Y, Liu R, Ikenoue T, Guan KL, Zheng P. TSC-mTOR maintains quiescence and function of hematopoietic stem cells by repressing mitochondrial biogenesis and reactive oxygen species. *J Exp Med*. 2008;205(10):2397–2408.
6. Chen C, Liu Y, Liu Y, Zheng P. mTOR regulation and therapeutic rejuvenation of aging hematopoietic stem cells. *Sci Signal*. 2009;2(98):ra75.
7. Young NS, Maciejewski J. The pathophysiology of acquired aplastic anemia. *N Engl J Med*. 1997;336(19):1365–1372.
8. Keeling DM, Isenberg DA. Haematological manifestations of systemic lupus erythematosus. *Blood Rev*. 1993;7(4):199–207.
9. Brunkow ME. Disruption of a new forkhead/winged-helix protein, scurfin, results in the fatal lymphoproliferative disorder of the scurfy mouse. *Nat Genet*. 2001;27(1):68–73.
10. Godfrey VL, Wilkinson JE, Rinchik EM, Russell LB. Fatal lymphoreticular disease in the scurfy (sf) mouse requires T cells that mature in a sf thymic environment: potential model for thymic education. *Proc Natl Acad Sci U S A*. 1991;88(13):5528–5532.
11. Kiel MJ, Yilmaz OH, Iwashita T, Yilmaz OH, Terhorst C, Morrison SJ. SLAM family receptors distinguish hematopoietic stem and progenitor cells and reveal endothelial niches for stem cells. *Cell*. 2005;121(7):1109–1121.
12. Wilson A, et al. Hematopoietic stem cells reversibly switch from dormancy to self-renewal during homeostasis and repair. *Cell*. 2008;135(6):1118–1129.
13. Bowie MB, McKnight KD, Kent DG, McCaffrey L, Hoodless PA, Eaves CJ. Hematopoietic stem cells proliferate until after birth and show a reversible phase-specific engraftment defect. *J Clin Invest*. 2006;116(10):2808–2816.
14. Malek TR, Danis KM, Codias EK. Tumor necrosis factor synergistically acts with IFN-gamma to regulate Ly-6A/E expression in T lymphocytes, thymocytes and bone marrow cells. *J Immunol*. 1989;142(6):1929–1936.
15. Poltorak A, et al. Defective LPS signaling in C3H/HeJ and C57BL/10ScCr mice: mutations in Tlr4 gene. *Science*. 1998;282(5396):2085–2088.
16. Boring L, et al. Impaired monocyte migration and reduced type 1 (Th1) cytokine responses in C-C chemokine receptor 2 knockout mice. *J Clin Invest*. 1997;100(10):2552–2561.
17. Bindl L, et al. Successful use of the new immunesuppressor sirolimus in IPEX (immune dysregulation, polyendocrinopathy, enteropathy, X-linked syndrome). *J Pediatr*. 2005;147(2):256–259.
18. Scadden DT. Stem cells and immune reconstitution in AIDS. *Blood Rev*. 2003;17(4):227–231.
19. Fuchs D, et al. Immune activation and the anaemia associated with chronic inflammatory disorders. *Eur J Haematol*. 1991;46(2):65–70.
20. Papadaki HA, et al. Increased apoptosis of bone marrow CD34(+) cells and impaired function of bone marrow stromal cells in patients with systemic lupus erythematosus. *Br J Haematol*. 2001;115(1):167–174.
21. Chang X, Zheng P, Liu Y. Selective Elimination of Autoreactive T cells in vivo by the Regulatory T Cells. *Clinical Immunology*. 2009;130(1):61–73.
22. Godfrey VL, Rouse BT, Wilkinson JE. Transplantation of T cell-mediated, lymphoreticular disease from the scurfy (sf) mouse. *Am J Pathol*. 1994;145(2):281–286.
23. Bacigalupo A, et al. Antilymphocyte globulin, cyclosporin, and granulocyte colony-stimulating factor in patients with acquired severe aplastic anemia (SAA): a pilot study of the EBMT SAA Working Party. *Blood*. 1995;85(5):1348–1353.
24. Bacigalupo A, et al. Antilymphocyte globulin, cyclosporine, prednisolone, and granulocyte colony-stimulating factor for severe aplastic anemia: an update of the GITMO/EBMT study on 100 patients. European Group for Blood and Marrow Transplantation (EBMT) Working Party on Severe Aplastic Anemia and the Gruppo Italiano Trapianti di Midolio Osseo (GITMO). *Blood*. 2000;95(6):1931–1934.
25. Rosenfeld SJ, Kimball J, Vining D, Young NS. Intensive immunosuppression with antithymocyte globulin and cyclosporine as treatment for severe acquired aplastic anemia. *Blood*. 1995;85(11):3058–3065.
26. Chang X, Zheng P, Liu Y. Homeostatic proliferation in mice with germline FoxP3 mutation and its contribution to fatal autoimmunity. *J Immunol*. 2008;181(4):2399–2406.
27. King C, Ilic A, Koelsch K, Sarvetnick N. Homeostatic expansion of T cells during immune insufficiency generates autoimmunity. *Cell*. 2004;117(2):265–277.
28. Rodriguez S, et al. Dysfunctional expansion of hematopoietic stem cells and block of myeloid differentiation in lethal sepsis. *Blood*. 2009;114(19):4064–4076.
29. Ueda Y, Kondo M, Kelsoe G. Inflammation and the reciprocal production of granulocytes and lymphocytes in bone marrow. *J Exp Med*. 2005;201(11):1771–1780.
30. Janeway CA. Approaching the asymptote? Evolution and revolution in immunology. *Cold Spring Harb Symp Quant Biol*. 1989;54 pt 1:1–13.
31. Matzinger P. Tolerance, danger, and the extended family. *Annu Rev Immunol*. 1994;12:991–1045.
32. Liu Y, Chen GY, Zheng P. CD24-Siglec G/10 discriminates danger- from pathogen-associated molecular patterns. *Trends Immunol*. 2009;30(12):557–561.
33. Chen GY, Tang J, Zheng P, Liu Y. CD24 and Siglec-10 selectively repress tissue damage-induced immune responses. *Science*. 2009;323(5922):1722–1725.
34. Lin W, et al. Regulatory T cell development in the absence of functional Foxp3. *Nat Immunol*. 2007;8(4):359–368.
35. Zhou H, et al. Generation of monoclonal antibodies against highly conserved antigens. *PLoS ONE*. 2009;4(6):e6087.